RSC Advances

PAPER

View Article Online
View Journal | View Issue

Cite this: *RSC Adv.*, 2021, **11**, 7294

Controllable enzymatic superactivity of α-chymotrypsin activated by the electrostatic interaction with cationic gemini surfactants†

Zheng Yue,‡[a] Meihuan Yao,‡[a] Guangyue Bai,*[a] Jiuxia Wang,[ab] Kelei Zhuo,[a] Jianji Wang[a] and Yujie Wang*[b]

Surfactant plays a critical role in enzymatic multi-functionalization processes. However, a deep understanding of surfactant-enzyme interactions has been lacking up until now due to the extreme complexity of the mixed system. This work reported the effect of cationic gemini surfactants, alkanediyl-α,ω-bis(dimethyldodecylammonium bromide) ($C_{12}C_SC_{12}Br_2$, $S = 2$, 6, and 10) on the enzymatic activity and conformation of α-chymotrypsin (α-CT) in phosphate buffer solution (PBS, pH 7.3). The enzymatic activity was assessed by the rate of 2-naphthyl acetate (2-NA) hydrolysis measured by UV-vis absorption. The superactivity of α-CT in the presence of $C_{12}C_SC_{12}Br_2$ appears in the concentration region below the critical micelle concentration (cmc) of the surfactant, and its maximum superactivity is correlated to the spacer length of $C_{12}C_SC_{12}Br_2$. Subtle regulation of the charge density of headgroups of the cationic surfactant can be achieved through partial charge neutralization of cationic headgroups by introducing inorganic counterions or oppositely charged surfactant, demonstrating that the electrostatic interaction plays the crucial role for emergence of the superactivity. The interaction between $C_{12}C_SC_{12}Br_2$ ($S = 2$,6, and 10) and α-CT was characterized by isothermal titration calorimetry (ITC), and the obtained endothermic enthalpy change indicates that the interaction induces the change in conformation and enzymatic superactivity. The methodologies of fluorescence spectroscopy, circular dichroism (CD), and differential scanning calorimetry (DSC) show that the gemini surfactants with different spacer lengths induct and regulate the secondary, tertiary and even fourth structures of the protein. The present work is significant to get deeper insight into the mechanism of the activation and denaturation of enzymes.

Received 19th November 2020
Accepted 7th February 2021

DOI: 10.1039/d0ra09843d

rsc.li/rsc-advances

1. Introduction

Hybrid systems of biological macromolecules and amphiphilic molecules have a wide range of applications in some science and technology fields, such as biomedicine, nanotechnology, pharmaceuticals and cosmetics.[1] Considerable effort has been made to study the interaction between protein and surfactant over the past few decades, which certainly promotes a deep understanding of the critical role of surfactant to the enzymatic multi-functionalization process. Herein the surfactant might be considered as a denaturant, activator or stabilizer and cross-linker, depending on the properties of both the studied surfactant and enzyme.[2] The highly regarded topics in the field in recent years are still focused on to explore how to maintain and enhance the activity and/or stability of enzymes.[3]

Alfa-chymotrypsin (α-CT) is often selected as a model enzyme of serine proteases in order to understand the mechanism on the interaction of surfactant with globular proteins in the presence of various types of surfactants, owing to the benefits of the enzyme's well-known structure and the mechanism of enzymatic reaction.[4–12] It is well known that anionic sodium dodecyl sulfate (SDS) can inhibit the activities of α-CT and many other globular proteins, and even can denature them, which makes it become a valuable denaturant. The electrostatic interaction of anionic SDS with the positively charged side chains of amino acid residues can be responsible to a large extent. The hydrophobic interaction between enzyme and SDS also promotes strongly the conformational changes by formation of enzyme/SDS complex. The thermodynamic analysis to their interactions provides much indispensable information for understanding deeply the effects of surfactant on the enzymatic reaction.[11,12]

It was noticed that some cationic surfactants can activate α-CT and some other enzymes in aqueous solvent, reverse micelle pool and microemulsion, as it has been reviewed recently.[2c,13,14]

[a]*Collaborative Innovation Center of Henan Province for Green Manufacturing of Fine Chemicals, Key Laboratory of Green Chemical Media and Reactions, Ministry of Education, School of Chemistry and Chemical Engineering, Henan Normal University, Xinxiang, Henan 453007, P. R. China. E-mail: baiguangyue@htu.cn*

[b]*School of Chemistry and Chemical Engineering, Henan Institute of Science And Technology, Xinxiang, Henan 453003, P. R. China. E-mail: yujiewang2001@163.com*

† Electronic supplementary information (ESI) available. See DOI: 10.1039/d0ra09843d

‡ Equal contribution, shared first authorship.

Cetyltrimethylammonium bromide (CTAB) inhibits the activity of α-CT for hydrolysis of *N*-glutaryl-L-phenylalanine *p*-nitroanilide (GPNA),[5–7] but it can activate the enzyme in 80% for catalyzing hydrolysis of the substrate *p*-nitrophenyl acetate (PNPA).[8] Dodecyltrimethylammonium bromide (DTAB) affects the catalytic activity of α-CT quite mildly for hydrolysis of 2-naphthyl acetate (2-NA),[15] but very strongly for hydrolysis of GPNA with a superactivity.[16] These results demonstrate the dependence of the enzyme activity on the substrate, which most likely stems from the different distribution of these substrates in micelle pseudophase. The substrates may be dissolved in the hydrophobic cores or the palisade layer of micellar assembles. Therefore, the accessibility of the enzyme to its substrate is a key factor in micellar solution,[1e] resulting in the substrate partition-dependent enzymatic activity.

Moreover, cetyltrialkylammonium bromide surfactants with different alkyl chain lengths from methyl to butyl have been used to study the enzyme α-CT activity.[6,7,13,17] A explicit conclusion is that the superactivity phenomenon becomes more pronounced with the increase in the side chain length from methyl to butyl, which is attributed to the enhancement of the headgroup's hydrophobicity.[6,7] Several other cationic surfactants with different headgroup structures, reported by Ghosh and Verma,[18] were used to activate the enzymatic hydrolysis of the substrate PNPA, as a result, the headgroup size affects intensely the enzymatic reaction rate. In the presence of dodecyltriphenylphosphonium bromide (DTPB) with largest headgroup size among their used surfactants, α-CT exhibits the highest superactivity. In practice, those apolar groups linked directly to the headgroup can increase both the headgroup's size and hydrophobicity.

The hydrophobic moiety of headgroups can enhance the van der Waals' interaction with the nearby hydrophobic amino residues and also affect the packing of the surfactant when the synergetic interaction of the surfactant occurs.[18–23] In dilute surfactant concentration range where the specific interaction occurs, the electrostatic attraction is the main factor controlling enzymatic activity.[7,24–26] The enzyme may retain its activity and even may exhibit a superactivity. According to these reported results, we can consider that the size effect of the surfactant headgroups reflects the restricted electrostatic interaction between enzyme and surfactant due to the steric effect. So far these effects are far from clear and further investigation is essential for the potential enzyme/surfactant applications.

To this end, the cationic gemini surfactant, alkanediyl-α,ω-bis(dimethylalkyl ammonium bromide) (designated as C_nC_S-C_nBr_2), is a good candidate to explore the effect of the electrostatic interaction on the enzymatic reaction since the change in the spacer length can adjust the charge density of the polar groups. Ones with short spacer have larger charge density than its monomer surfactant. Therefore, the gemini $C_nC_SC_nBr_2$ with short spacer ($S \leq 6$) can interact more efficiently with proteins, such as bovine serum albumin (BSA)[27] and myoglobin.[28] Ones with long spacer behave more like two surfactant molecules linked with a hydrophobic linker in the terms of the charge density.[27,29–31] The α-CT activity in aqueous media has been studied in the presence of $C_{16}C_SC_{16}Br_2$ (S = 3, 6, 10,12).[32] The results show that the enzyme has the higher activity as compared to CTAB. The highest superactivity was obtained in the presence of $C_{16}C_{12}C_{16}Br_2$, but its effect on the enzyme structures still remains unclear. On the other hand, it is worth noting that some gemini surfactants with double cetyl chains can be used only in a limited concentration range due to their higher Kraft points.[31]

In the terms of the enzyme structures, a comparable study is that DTAB makes only subtle changes in the protein structure, whereas the more hydrophobic CTAB and octadecyltrimethylammonium bromide (OTAB) induce an incontestable unfolding.[33] When the hydrophobic chain is cut to very short length, tetrabutylammonium bromide (TBABr) only induces much smaller change in the protein conformation, which confirms the effect of the hydrophobic moieties of cationic surfactants.[34] In our recent work,[26] the gemini surfactant $C_{12}C_{10}C_{12}Br_2$ with a low Kraft point was used to activate α-CT. It is evidenced that the enzyme has a flexible and unstable conformation when it exhibits a superactivity. It may induce protein flexibility, but not unfolding. However, it is still unclear how the structure of α-CT will change with the electrostatic interaction due to the change in the charge density of a surfactant headgroup.

On the basis of the weaker hydrophobic efficiency of dodecyl chain[33] and its lower Kraft points,[31] compared with $C_{16}C_SC_{16}Br_2$ having cetyl chains as mentioned above, in present work, we chose $C_{12}C_SC_{12}Br_2$ having typical three spacer lengths of S = 2, 6 and 10 to explore how the distance between the two positive headgroups or the headgroup's charge density affects the activity of α-CT and its structures. The charge density of the headgroups also was controlled by partial charge neutralization with some kinds of counterions. The interactions between the cationic gemini surfactant and α-CT were characterized by enzymatic activity assessment, ITC, fluorescence spectroscopy, CD spectroscopy and DSC. This work is going to provide a valuable insight into the relationship of surfactant structure with activity regulation of protein molecules.

2. Results and discussion

2.1 Relative activity of α-CT in cationic surfactant solution

2.1.1 The effects of spacer chain length of gemini surfactants. The hydrolysis of 2-NA catalyzed by α-CT was conducted at the constant concentrations of 0.10 g L^{-1} α-CT, 0.081 mmol L^{-1} 2-NA, 3% (volume) glycol and 10 mmol L^{-1} PBS (pH 7.3) and at various surfactant concentrations. The initial rate was obtained by the initial slope of the curve of concentration of 2 N produced under catalysis of α-CT as a function of time, and three typical curves in the presence of $C_{12}C_{10}C_{12}Br_2$ were shown in Fig. S1.† The presented relative activity (ν_r) of α-CT was expressed as a ratio of the initial hydrolysis rate (ν_i) in the buffered surfactant solution to the initial rate (ν_{PBS}) in pure PBS and the standard deviation evaluated is ±0.03. The variation of ν_r with the concentration ratio (C_i/cmc$_i$) of $C_{12}C_SC_{12}Br_2$ (S = 2, 6, and 10) or DTAB in 10 mmol L^{-1} PBS was shown in Fig. 1, where the ratio C_i/cmc$_i$ was used for clearly distinguishing the effect of surfactant monomers and micelles on the enzymatic activity.

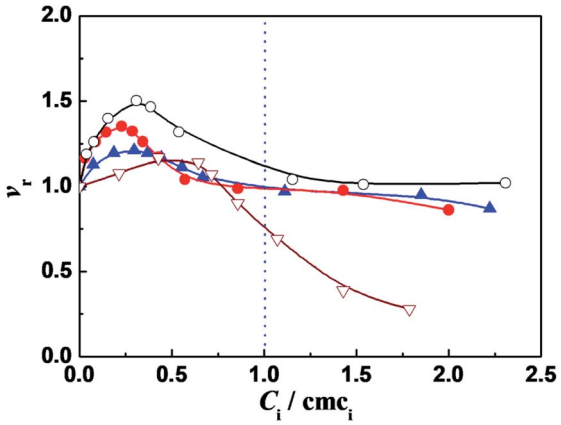

Fig. 1 Variation of the relative activity (ν_r) of α-CT with the ratio of concentration to cmc (C_i/cmc$_i$) of: $C_{12}C_2C_{12}Br_2$ (▲), $C_{12}C_6C_{12}Br_2$ (●), $C_{12}C_{10}C_{12}Br_2$ (○) and DTAB (▽), respectively. The concentrations of other components are 0.10 g L^{-1} α-CT, 0.081 mmol L^{-1} 2-NA, 10 mmol L^{-1} PBS (pH 7.3) and 3 (*v*/*v*)% glycol, respectively. The enzyme was incubated for 10 min in the surfactant solution before 2-NA was added to trigger the enzymatic reaction.

The reaction was triggered by adding 2-NA after incubated for 10 min in the buffered surfactant solution.

It was found that in the surfactant monomer solutions (C_i/cmc$_i$ < 1), the ν_r values of enzymatic reaction are larger than one, going through a maximum value ν_{max} as the ratio C_i/cmc$_i$ increases (Fig. 1). The enzymatic superactivity appears even at the first addition (such as 5 μM for $C_{12}C_{10}C_{12}Br_2$). The cmc values in 10 mmol L^{-1} PBS (pH = 7.3), obtained from ITC (Table 1, see the Section 2.2), are 0.27, 0.35, 0.13 and 14.0 mmol L^{-1} for $C_{12}C_SC_{12}Br_2$ (S = 2, 6, 10) and DTAB, respectively, and the surfactant concentrations at which the maximum ν_r values appear correspond to 0.070 mmol L^{-1} (0.26 cmc), 0.081 mmol L^{-1} (0.23 cmc), 0.040 mmol L^{-1} (0.31 cmc) and 7.84 mmol L^{-1} (0.56 cmc), respectively. In comparison, for $C_{12}C_2C_{12}Br_2$ the short spacer length with the two methylenes draws the two positive charges close, which leads to a high charge density of the headgroups and the enhanced electrostatic interaction with the negative sites of protein. The two headgroups of $C_{12}C_6C_{12}Br_2$ have a separation similar to the length between two closely packed DTAB molecules,[31] hence the electrostatic interaction with the negative sites of protein is weaker than that in the case of $C_{12}C_2C_{12}Br_2$. For $C_{12}C_{10}C_{12}Br_2$ each headgroup has a charge density just like a single headgroup but the distance between the two charges is restricted by flexible methylene spacer. Because of the equal hydrophobic chain length (C_{12}) for every surfactant, the differences in the α-CT activities in Fig. 1 can be attributed mainly to the extent of electrostatic interaction induced by changing the spacer chain length.

Table 1 Thermodynamic parameters of micellization for $C_{12}C_SC_{12}Br_2$ and DTAB in PBS at T = 298.15 ± 0.01 K[a]

Surfactant	C_{buffer} (mmol L^{-1})	cmc (mmol L^{-1})	ΔH_{mic} (kJ mol^{-1})
$C_{12}C_2C_{12}Br_2$	10	0.27 ± 0.01	−7.1 ± 0.3
$C_{12}C_6C_{12}Br_2$	10	0.35 ± 0.01	−3.9 ± 0.1
	30	0.27 ± 0.01	−3.1 ± 0.3
	50	0.25 ± 0.01	−2.6 ± 0.1
	70	0.19 ± 0.01	−2.1 ± 0.1
$C_{12}C_{10}C_{12}Br_2$	10	0.13 ± 0.02	−4.7 ± 0.2
DTAB	10	14.6 ± 0.2	−2.0 ± 0.3

[a] Note: the values (cmc and ΔH_{mic}) were directly derived from ITC measurements (see ESI: Fig. S5 and S6); the standard uncertainties of cmc and ΔH_{mic} were provided in the table, respectively.

Further, the ν_r values tend to one after the cmc values of these gemini surfactants (C_i/cmc$_i$ > 1). A reasonable factor is the decrease in the effective 2-NA concentration owing to some 2-NA dissolving into the micellar pseudophase.[15] The spectra of 2-NA shift to red after the cmc values of $C_{12}C_SC_{12}Br_2$ (Fig. S2†), suggesting that some 2-NA molecules locate in the less hydrophilic palisade layer of the micelles. On the other hand, the product 2 N also prefers to dissolve in the micelle pseudophase just like 2-NA (Fig. S3†).

The maximum relative activities obtained from Fig. 1 are $\nu_{r,max}$ = 1.2, 1.35, 1.5 for $C_{12}C_SC_{12}Br_2$ (S = 2, 6, 10) and 1.2 for DTAB, respectively, indicating that the superactivity of α-CT is correlated with the methylene chain length S of the spacer. Therefore, it is possible that the charge density of the headgroups mainly affects the superactivity. On the other hand, it can be known that the molar ratios of $C_{12}C_2C_{12}Br_2$, $C_{12}C_6C_{12}Br_2$, and $C_{12}C_{10}C_{12}Br_2$ to α-CT (0.1 g L^{-1}) at the maximum α-CT activity are approximate to 18, 20, and 10, respectively, and in comparison the number of the negatively charged amino acid residues for each α-CT[35] is 13, suggesting that most of the gemini molecules are attached on the enzyme surface possibly by the electrostatic interaction. It has relevance to the conclusion that the hydrophobicity or size of the cationic headgroups can affect the superactivity of α-CT.[6,7,18]

2.1.2 Subtle regulation on the charge density of headgroups of cationic surfactant. In order to explore the relationship between the charge density of the positive headgroups for every surfactant and the α-CT activity, an available method for changing the charge density is to neutralize partially the headgroup charge by adding inorganic counterion or anionic surfactant. The phosphate buffer system (pH 7.3), which acts in the cytoplasm of all cells, consists of $H_2PO_4^-$ as proton donor and HPO_4^{2-} as proton acceptor:

$$H_2PO_4^- \rightleftharpoons H^+ + HPO_4^{2-} \quad (1)$$

and a simultaneous balance with a cationic surfactant occurs as

$$HPO_4^{2-} + R(CH_3)_3N^+ \rightleftharpoons \left(R(CH_3)_3N^+HPO_4^{2-}\right)^- \quad (2)$$

where we ignore the interaction of the cationic surfactant with $H_2PO_4^-$. The interaction described in eqn (2) was confirmed by titrating the buffered surfactant into the same buffer solution, leading to a pronounced decrease in the specific conductivity in a dilute surfactant concentration range (Fig. S4†). The non-covalent electrostatic association can reduce the average charge density of the surfactant headgroup, and consequently would change the effect of the surfactant on the relative activity of α-CT. The zeta-potential measurements of α-CT gave small negative values below −10 mV (Table S3†) unchanged almost

with PBS concentration, suggesting that the effect of PBS on the interaction between α-CT and cationic gemini surfactants sterns mainly from the change in the charge density of the surfactant headgroups.

We did choose the specific surfactant concentration at which the maximum superactivity appears in Fig. 1 to explore the effect of PBS concentration (C_{buffer}) on the relative activity of α-CT. Thus the variation of relative activity (v_r) of α-CT with the C_{buffer} was presented in Fig. 2, where the relative activity was expressed as the ratio of the initial hydrolysis rate in the presence of buffered surfactant to the rate in its corresponding PBS concentration. The buffer concentration corresponding to the maximum activity ($v_{r,max}$) is 10–20 mmol L^{-1} ($v_{r,max} = 1.52$) for $C_{12}C_{10}C_{12}Br_2$, 50 mmol L^{-1} ($v_{r,max} = 1.70$) for $C_{12}C_6C_{12}Br_2$, 60 mmol L^{-1} ($v_{r,max} = 1.59$) for $C_{12}C_2C_{12}Br_2$ and 50 mmol L^{-1} ($v_{r,max} = 1.55$) for DTAB used as a reference (Fig. 2), respectively, which is consistent to the order of the increased charge density of the $C_{12}C_SC_{12}Br_2$ headgroups. The results suggest that the partial charge neutralization of the cationic surfactant is advantageous to activating α-CT to some extent. The surfactant with a shorter spacer chain or a larger charge density can activate the maximum relative activity in a much concentrated buffer solution. It is worth noting that the used concentration of every surfactant in Fig. 2 is below its cmc value in the corresponding buffer solution (Table 1, see the Section 2.2) and the superactivity appears before these cmc values. Therefore, the variation of α-CT activity with PBS concentration in the presence of $C_{12}C_SC_{12}Br_2$ results from the change in the headgroup's charge density. Further the reduced electrostatic attraction between the surfactant and α-CT is benefit for increasing α-CT activity. These results mean that the enzymatic activity can be controlled by adjusting the charge density of surfactant headgroup.

Another way to neutralize partially the charge of the headgroups is to add an oppositely charged surfactant. Fig. 3 shows the variation of α-CT relative activity v_r with the molar fraction of anionic surfactant SDS (x_{SDS}) in the mixture of the cationic surfactant and SDS. For every system in Fig. 3, the cationic surfactant has a constant concentration and SDS component increases to cover the studied molar fraction. The cationic surfactant concentrations in Fig. 3 were identical to the values in Fig. 2. The v_r value decreases as x_{SDS} increases for the mixed $C_{12}C_{10}C_{12}Br_2$/SDS, and has an extreme value at $x_{SDS} = 0.05$ for $C_{12}C_6C_{12}Br_2$/SDS, and a plateau after $x_{SDS} = 0.20$ for $C_{12}C_2C_{12}Br_2$/SDS, respectively. However, for every mixture of the studied cationic surfactant and SDS, especially for DTAB and SDS, the activity was only assessed in a narrow component range due to the transition of their aggregate morphologies from micelle solution to turbid multiphase systems with big aggregates, and pure SDS will denature α-CT even at a dilute concentration[11,12]

Both SDS and $C_{12}C_SC_{12}Br_2$ ionize completely into surfactant ions and the corresponding counterions in aqueous solution before their respective cmc values. In a mixture of SDS and $C_{12}C_SC_{12}Br_2$, the anionic DS^- from SDS and the cationic $C_{12}C_SC_{12}^{2+}$ from $C_{12}C_SC_{12}Br_2$ would interact electrostatically to form $C_{12}C_SC_{12}^{2+}\cdot DS^-$ complex at $x_{12\text{-}S\text{-}12} \gg x_{SDS}$ before their mixed cmc. In our previous study, it was proved by ITC that this kind of ionic pair complex did form, following a large negative enthalpy change of interaction,[36] and by the conductivity measurements, following a decrease in conductivity after adding SDS into $C_{12}C_SC_{12}Br_2$-rich solutions.[37] The partial neutralization of $C_{12}C_SC_{12}^{2+}$ should lower the average charge density of $C_{12}C_SC_{12}Br_2$ headgroups and weaken the interaction between $C_{12}C_SC_{12}Br_2$ and α-CT. Similarly to the effect of phosphate buffer, the surfactant with a larger charge density needs a larger x_{SDS} for activating the maximum relative activity.

We can conclude that the cationic surfactants may induce the superactivity of α-CT, and the variation of the relative activity of α-CT is correlated to the spacer length of gemini

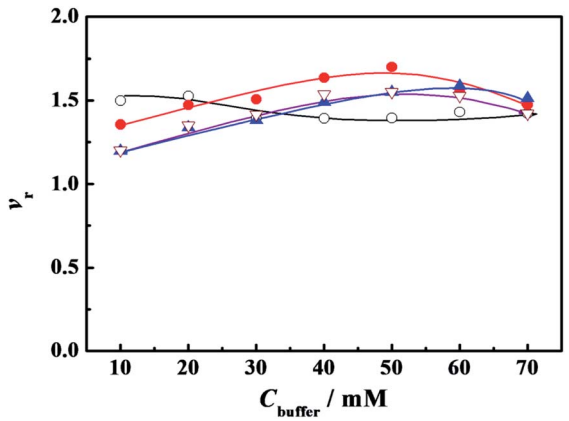

Fig. 2 Variation of the relative activity (v_r) of α-CT with the concentration of phosphate buffer (C_{buffer}). The symbols indicate the surfactant: (▲) $C_{12}C_2C_{12}Br_2$ (0.07 mmol L^{-1}), (●) $C_{12}C_6C_{12}Br_2$ (0.08 mmol L^{-1}), (○) $C_{12}C_{10}C_{12}Br_2$ (0.04 mmol L^{-1}) and (▽) DTAB (6.0 mmol L^{-1}), respectively. The concentrations of other components were 0.10 g L^{-1} α-CT, 0.081 mmol L^{-1} 2-NA and 3 (*v*/*v*)% glycol, respectively. The α-CT was incubated for 10 minutes before 2-NA was added for all the experiments.

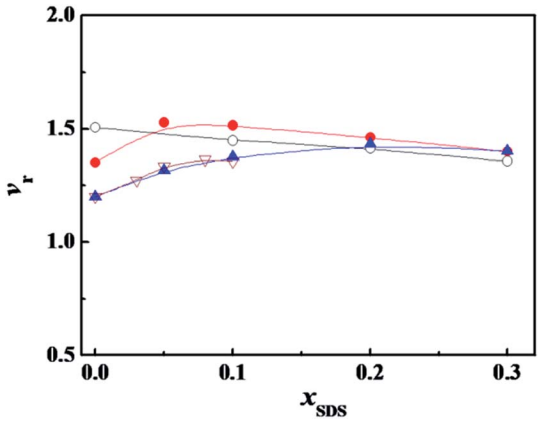

Fig. 3 Variation of the relative activity (v_r) of α-CT with the molar fraction of SDS (x_{SDS}) in the mixture of SDS with (▲) $C_{12}C_2C_{12}Br_2$ (0.07 mmol L^{-1}), (●) $C_{12}C_6C_{12}Br_2$ (0.08 mmol L^{-1}), (○) $C_{12}C_{10}C_{12}Br_2$ (0.04 mmol L^{-1}) and (▽) DTAB (6.0 mmol L^{-1}), respectively. The concentrations of the other components were 0.10 g L^{-1} α-CT, 10 mmol L^{-1} PBS, 0.081 mmol L^{-1} 2-NA and 3 (*v*/*v*)% glycol, respectively. The α-CT was incubated for 10 minutes before 2-NA was added for all the experiments.

surfactant. In particular, the charge density of headgroups of the cationic surfactant may be adjusted by neutralizing partially the headgroup charge with adding inorganic counterion or anionic surfactant, as a result, the maximum activity can be controlled by the electrostatic interaction.

2.2 Calorimetric study on interaction of α-CT with $C_{12}C_SC_{12}Br_2$

ITC is a direct methodology to study thermodynamics of molecular self-assembly of surfactant in aqueous solution in terms of the enthalpy change as a function of surfactant concentration in calorimetric cell, since it can provide an extensive profile of the different intermolecular interaction steps by titrating small aliquots of a titrant.[36] When the concentrated $C_{12}C_SC_{12}Br_2$(S = 2, 6, and 10) or DTAB solution was titrated into 10 mmol L^{-1} phosphate buffer solutions, the cmc values and the corresponding enthalpies of micellization (ΔH_{mic}) can be obtained by ITC, as shown in Fig. S5† and listed in Table 1. The cmc values and exothermic micellization enthalpies for $C_{12}C_SC_{12}Br_2$ are lower in PBS (pH = 7.3) than in pure water,.[36b] The results might stem together from the effects of ionic strength and the partial charge neutralization of $C_{12}C_SC_{12}Br_2$ with phosphate anions (electrostatic attraction). The cmc values for DTAB present the almost equal values in pure water[36a] and in 10 mmol L^{-1} PBS.

It was found that the obvious interaction between the surfactant $C_{12}C_{10}C_{12}Br_2$ and α-CT occurs below its cmc,[26] and in this work the same event occurred for the studied $C_{12}C_2C_{12}Br_2$ and $C_{12}C_6C_{12}Br_2$, as shown in Fig. S6.† Then our following interest is focused on the interaction in dilute concentration range. Thus the difference ($\Delta(\Delta H_{obs})$) between the observed enthalpies in the presence of α-CT and in its absence, shown in Fig. 4, can highlight the total enthalpy change resulted from the interaction of surfactant with α-CT, including the effects in electrostatic attraction (exothermic),[15] van der Waals attractions (exothermic), release of combined water (endothermic) and conformational change (endothermic) of α-CT. Except for the case titrated by DTAB, the curves go through an extreme for every gemini surfactant and rise up following the increase in α-CT concentration. The positive $\Delta(\Delta H_{obs})$ value means a neat endothermic interaction between the surfactant and α-CT, suggesting that the $\Delta(\Delta H_{obs})$ mainly arises from the dehydration and enzyme conformation change. Such endothermic effect was also observed for protein unfolding in the presence of surfactant in previous works.[1b,38] The larger the positive $\Delta(\Delta H_{obs})$ value is, the larger the enthalpy change associated with the conformational change is or the smaller the electrostatic attraction is. Therefore, the increase in $\Delta(\Delta H_{obs})$ values in the order of $C_{12}C_2C_{12}Br_2$, $C_{12}C_6C_{12}Br_2$ and $C_{12}C_{10}C_{12}Br_2$ results most possibly from the decrease in their headgroup's charge densities. Therefore, there is an entropy-driven interaction between the surfactants and α-CT. The entropy gains mainly stem from the change in the conformation of α-CT and the release of the some water molecules attached on the surfactant molecules and the enzyme surface. It is interesting that the trend is consistent with the change of the enzyme relative activities in the presence of the surfactant (Fig. 1). The maximum $\Delta(\Delta H_{obs})$ appears in the C_i/cmc range where α-CT behaves superactivity in the individual surfactant solution.

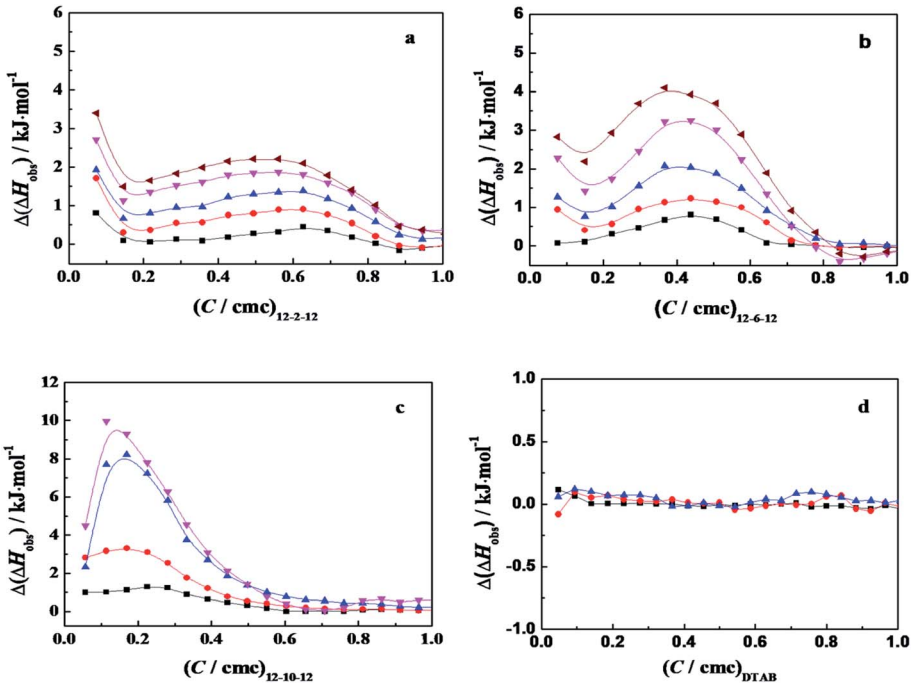

Fig. 4 The plots of $\Delta(\Delta H_{obs})$ as a function of the concentration ratios (C/cmc) of $C_{12}C_SC_{12}Br_2$ (S = 2, 6 and 10) and DTAB for titrating α-CT solution with: (a) $C_{12}C_2C_{12}Br_2$, (b) $C_{12}C_6C_{12}Br_2$, (c) $C_{12}C_{10}C_{12}Br_2$, and (d) DTAB. The symbols mark the α-CT concentration (g L^{-1}) of: (■) 0.05; (●) 0.10; (▲) 0.20; (▼) 0.30; and (◀) 0.40, respectively, in 10 mmol L^{-1} PBS (pH 7.3). The concentration in the syringe is 3.0 mmol L^{-1} for $C_{12}C_2C_{12}Br_2$, 4.0 mmol L^{-1} for $C_{12}C_6C_{12}Br_2$, 2.0 mmol L^{-1} for $C_{12}C_{10}C_{12}Br_2$ and 200 mmol L^{-1} for DTAB, respectively.

The effect of PBS concentration on the enthalpy of interaction between surfactant and α-CT can be characterized by ITC. Variation of the observed enthalpy with $C_{12}C_6C_{12}Br_2$ concentration under different PBS concentrations in the presence of α-CT and in its absence was shown in Fig. S7.† Fig. 5 exhibits the differences ($\Delta(\Delta H_{obs})$) of the observed enthalpies in the presence of α-CT and in its absence in the dilute concentration range of $C_{12}C_6C_{12}Br_2$, which highlights the interaction of $C_{12}C_6C_{12}Br_2$ with α-CT at four PBS concentrations. The maximum $\Delta(\Delta H_{obs})$ values decrease as PBS concentration increases from 10 to 70 mmol L^{-1}, indicating that the decrease in charge density through the partial charge neutralization weakens the attractive interaction between $C_{12}C_6C_{12}Br_2$ and α-CT. In comparison with the change tendency of relative activity in Fig. 2, the enzymatic activity correlates closely with the enthalpy of interaction. It is worth noting that a moderate enthalpy change of interaction is benefit to activate α-CT for the mixed α-CT/cationic surfactant systems.

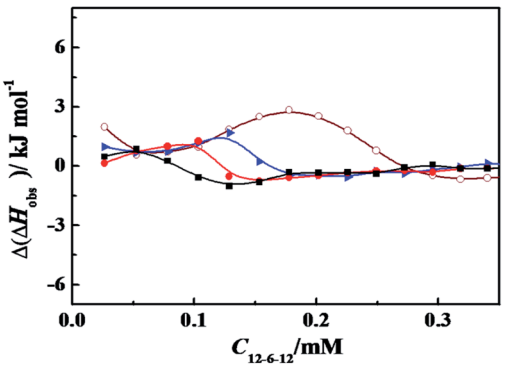

Fig. 5 The plots of $\Delta(\Delta H_{obs})$ as a function of $C_{12}C_6C_{12}Br_2$ concentration for titrating $C_{12}C_6C_{12}Br_2$ into 0.30 g L^{-1} α-CT solution at 298.15 K. The symbols mark the PBS (pH = 7.3) concentration (mmol L^{-1}) of (○) 10; (▶) 30; (●) 50; and (■) 70, respectively. The concentration of $C_{12}C_6C_{12}Br_2$ is 4.0 mmol L^{-1} in the syringe.

2.3 Fluorescence measurement

For understanding the effect on the tertiary structure of α-CT of interaction between $C_{12}C_SC_{12}Br_2$ or DTAB and α-CT, the fluorescence spectra of α-CT were acquired at an excitation wavelength of 295 nm, which reflects the change of the microenvironment around the aromatic Trp residues.[8,39] Fig. 6 shows the spectra after incubated for 10 min, respectively, in $C_{12}C_SC_{12}Br_2$ ($S = 2$, 6 and 10) or DTAB solutions with different concentrations and one typical spectrum after incubated for 120 min extracted from Fig. S8.†

The maximum wavelength (λ_{max}) of α-CT fluorescence is 338 nm in PBS, and the surfactants result in two changes in the fluorescence spectra, increase in fluorescence intensity and wavelength redshift. The increased fluorescence intensity stems from the decrease in its internal quenching effect,[8] indicating that α-CT has a more flexible conformation in the presence of

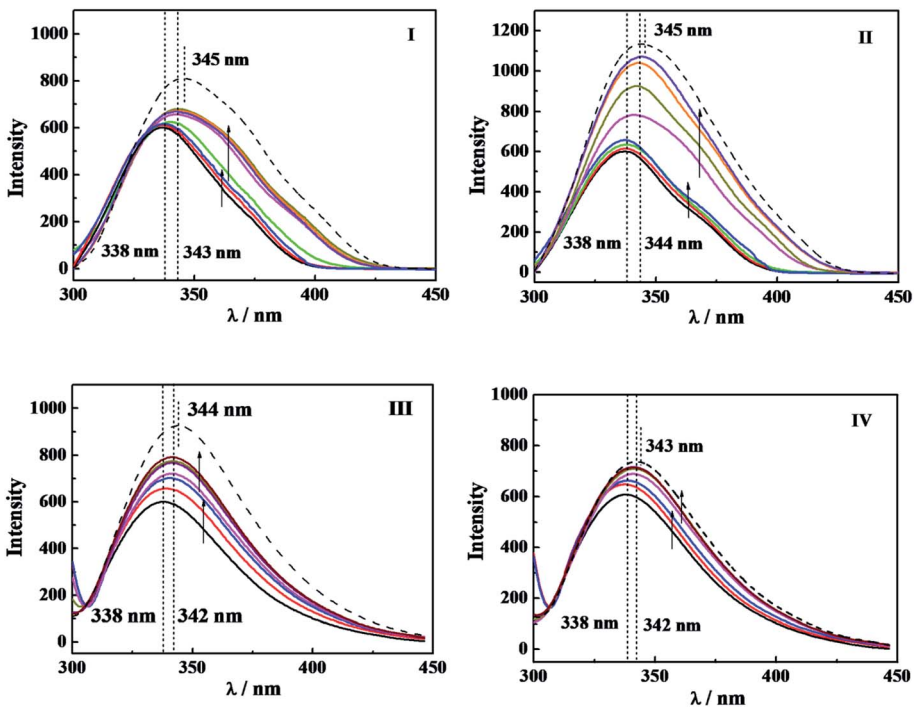

Fig. 6 The fluorescence spectra of 0.10 g L^{-1} α-CT at 298.2 K in (I) $C_{12}C_2C_{12}Br_2$ solution of 0, 0.03, 0.06, 0.15, 0.30, 0.60, 1.20 and 2.10 mmol L^{-1}, after incubating 10 min, and 2.10 mmol L^{-1} after incubating 120 min (dash), respectively; (II) $C_{12}C_6C_{12}Br_2$ solution of 0, 0.05, 0.10, 0.20, 0.40, 0.80, 1.60, and 2.00 mmol L^{-1}, after incubating 10 min, and 2.00 mmol L^{-1} after incubating 120 min (dash), respectively; (III) $C_{12}C_{10}C_{12}Br_2$ solution of 0, 0.05, 0.10, 0.20, 0.40, 0.80 and 1.50 mmol L^{-1}, after incubating 10 min, and 1.50 mmol L^{-1} after incubating 120 min (dash), respectively; (IV) DTAB solution of 0, 5.0, 10.0, 15.0, 20.0, 25.0 and 30.0 mmol L^{-1}, after incubating 10 min, and 30.0, mmol L^{-1} after incubating 120 min (dash), respectively. The arrows indicate the direction of the concentration increase before and after cmc, respectively.

the surfactants, which brings about a far distance of Trp from some other residues, such as Arg, due to the effect of $C_{12}C_SC_{12}Br_2$. The wavelength redshifts arise from the change in the environmental polarity around its Trp residues due to their partial expose to aqueous solvent. Before the respective cmc for the four surfactants, the fluorescence intensity rises up along with the constant λ_{max}, while after the cmc, the increase in the intensity and the redshift in the wavelength simultaneously occur. Therefore, it may demonstrate that α-CT has more flexible tertiary structure before the cmc of gemini surfactants and takes partial unfolding of the tertiary structure after their cmc values. However, the change in fluorescence intensity is too small to compare the extent among the different surfactants before their cmc values. When the incubation time was increased to 120 min as shown in Fig. S8† and in Fig. 6 (dash line), a small further redshift and significant increase in fluorescence intensity appear. In the extended incubation period after 3 h the further redshift and decreased fluorescence intensity occur (see short dash curve in Fig. S8†). These results indicate the dynamic instability of the tertiary structure of α-CT in the presence of the cationic surfactants.

In comparison of the fluorescence results with the relative activity in Fig. 1 and the interaction enthalpy in Fig. 4, one can understand that (i) the large superactivity of α-CT in the presence of the cationic surfactants corresponds to the gentle change in the tertiary conformation before cmc; (ii) after the cmc the relative activity reduces significantly, probably reflecting combining contributions from the distribution of 2-NA in the micelles and the tertiary conformation change; (iii) the increase in $\Delta(\Delta H_{obs})$ with the spacer length (Fig. 4) should relate to the conformational change besides the electrostatic attraction. As a reference, the effect of DTAB always deviates from the orders induced by the gemini surfactants in the respects of the enzymatic activity, $\Delta(\Delta H_{obs})$ and the tertiary structure, the most possible reason is its single head-tail structure and also its much larger cmc.

2.4 CD spectroscopy

Circular dichroism spectroscopy is a widely used technique for examining protein secondary structure. α-CT is a type of β-II proteins whose spectrum resembles that of random coil conformation, owing to their low β-sheet/PP-II-helix ratios.[40] Crystal structure data show that this kind of protein consists of antiparallel pleated β-sheets which are highly distorted or form very short irregular strands. This may cause the negative CD band to shift from the ideal β-sheet position (210–220 nm) towards the 200 nm region.[41]

The conformational changes of α-CT induced by $C_{12}C_SC_{12}Br_2$ ($S = 2$, 6, and 10) were characterized by using CD spectroscopy, as shown in Fig. 7. The CD spectrum of native α-CT in PBS shows a negative band with a minimum at 201 nm and an indistinct band at 230 nm. The bands of the spectra at 201 nm of α-CT incubated in $C_{12}C_SC_{12}Br_2$ solution present more negative extreme and unchanged wavelength before its cmc. After the cmc, the enhancement and redshift of the negative band occur simultaneously. The conformational components of the secondary structure were quantified by analyzing the CD spectra with CDNN software, as given in Table 2. The percentage of α-

Table 2 Secondary structure components of α-CT (0.10 g L^{-1}) incubated for 10 min in $C_{12}C_SC_{12}Br_2$ solution from far-UV CD spectra at 298 K

C_i (mmol L^{-1})	C_i/cmc	α-helix (%)	β-sheet (%)	β-turns (%)	Random coil (%)
PBS (10 mmol L^{-1}, pH = 7.3)					
0	0	7.0	41.9	19.9	32.7
$C_{12}C_2C_{12}Br_2$					
0.06	0.22	7.0	39.8	20.4	33.6
0.15	0.56	7.0	39.1	20.5	33.8
0.30	1.11	7.4	40.8	20.6	32.7
0.60	2.22	7.5	39.2	20.9	33.2
1.20	4.44	8.3	41.4	20.7	31.6
$C_{12}C_6C_{12}Br_2$					
0.05	0.14	7.0	39.7	20.4	33.6
0.10	0.29	6.9	38.5	20.6	34.1
0.20	0.57	7.0	38.5	20.8	34.0
0.80	2.29	7.3	38.9	21.1	33.6
1.60	4.57	7.2	41.9	20.3	32.6
$C_{12}C_{10}C_{12}Br_2$					
0.02	0.15	6.7	39.9	20.3	33.6
0.04	0.31	6.7	38.4	20.6	34.3
0.08	0.62	6.8	36.9	20.9	34.8
0.16	1.23	6.8	38.4	20.7	34.1
0.60	4.62	6.9	38.2	21.0	34.1

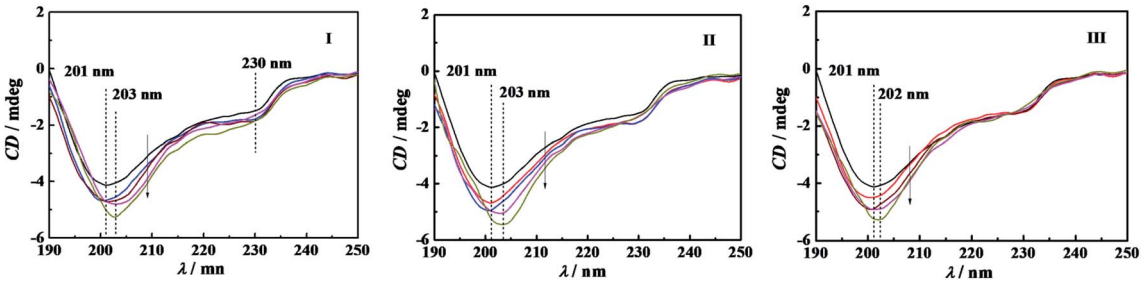

Fig. 7 Far-UV CD spectra of 0.10 g L^{-1} α-CT incubated for 10 min in buffer and buffered $C_{12}C_SC_{12}Br_2$ at the respective concentration (mmol L^{-1}) of (I) $C_{12}C_2C_{12}Br_2$: 0, 0.06, 0.15, 0.3,0.6, respectively; (II) $C_{12}C_6C_{12}Br_2$: 0, 0.05, 0.1, 0.5,0.8, respectively; and (III) $C_{12}C_{10}C_{12}Br_2$: 0, 0.02, 0.04, 0.16, 0.6, respectively. The arrow points to the direction of the concentration increment. The PBS has a concentration of 10 mmol L^{-1} and pH d7.3.

helix and β-sheet of α-CT in 10 mmol L^{-1} buffer is 7.0% and 41.9%, respectively. Attri, *et al.* found that the secondary structure composition of α-CT in 0.05 mol L^{-1} Tris–HCl buffer (pH 8.20) is 8% α-helix and 45% β-sheet,[42] and in 40 mM Tris/HCl (pH 7.0) buffer a β-sheet content of 47% from Simon.[43] For the cases in $C_{12}C_2C_{12}Br_2$ and $C_{12}C_6C_{12}Br_2$ solutions the percentages of α-helix and β-sheet slightly increase after their cmc. However, the percentages of α-helix and β-sheet in buffered $C_{12}C_{10}C_{12}Br_2$ are lower than in pure PBS in the studied concentration range, which corresponds well to those events, as mentioned above for this surfactant, identified by the superactivity, interaction enthalpy, and fluorescence spectrum. In addition, before the cmc values of $C_{12}C_SC_{12}Br_2$ (S = 2, 6, 10) the percentage of random coil increases slightly owing to the transition from the other order structures. In comparison with the conformational components in pure PBS, the change in secondary structure of α-CT before the individual cmc of the gemini surfactants is unconspicuous and doesn't seem to be the main factors affecting the enzyme activity. It is difficult to acquire a well-defined CD spectrum of α-CT in DTAB solution with the high concentration as employed in the other experiments due to the effect of Br^-.

2.5 Thermal stability of α-CT

A powerful tool for investigation on thermodynamic stability of protein is differential scanning calorimetry (DSC). The curve of the heat capacity of protein *versus* temperature undergoes commonly a sharp endothermic peak when the protein transits from its native to an unfolding or denatured state.[42,44] The identification of transition enthalpy (ΔH) and transition temperature (T_m) are helpful to understand the thermal stability

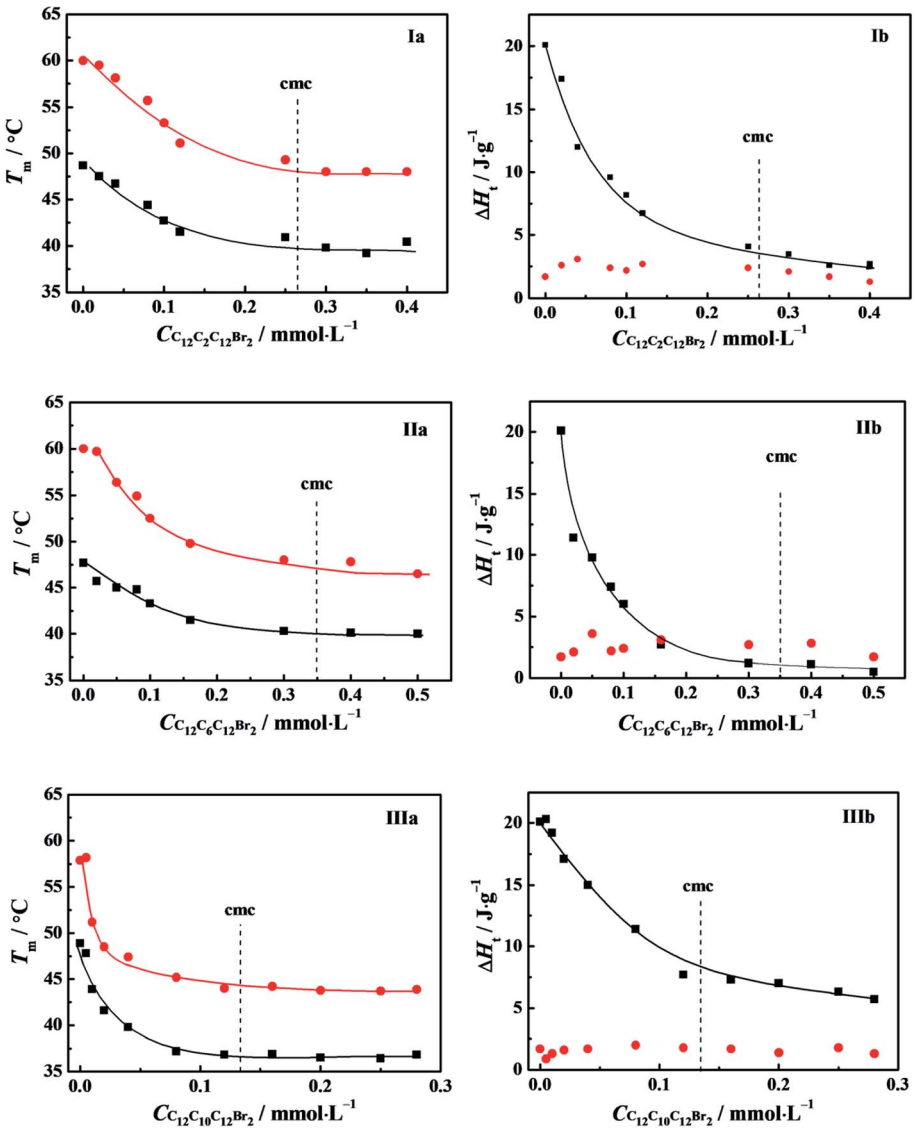

Fig. 8 Variation of the transition temperatures (a) and corresponding enthalpy changes (b) with the concentration of: (I) $C_{12}C_2C_{12}Br_2$, (II) $C_{12}C_6C_{12}Br_2$ and (III) $C_{12}C_{10}C_{12}Br_2$. The symbols mark (■) $T_{m,1}$, (●) $T_{m,2}$, (■) ΔH_1, (●) ΔH_2, respectively. The α-CT solution of 0.5 g L^{-1} was incubated for 20 min in 10 mmol L^{-1} PBS or buffered $C_{12}C_SC_{12}Br_2$. The data of IIIa and IIIb for $C_{12}C_{10}C_{12}Br_2$ are from the ref. [26].

of α-CT in $C_{12}C_SC_{12}Br_2$ ($S = 2$, 6, and 10) solutions and even the interaction between α-CT and $C_{12}C_SC_{12}Br_2$.

DSC thermograms obtained for α-CT in the presence of $C_{12}C_SC_{12}Br_2$ ($S = 2$, 6) were shown in Fig. S9.† The thermograms show two endothermic peaks, suggesting a thermal denaturation process with multi-transitions. The both corresponding transition temperatures are expressed as $T_{m,1}$ and $T_{m,2}$, respectively. The curves can be fitted by Gaussian function[26] to obtain the contribution of each component to total transition enthalpy. All the transition temperatures and corresponding enthalpy changes for the studied systems were collected in Tables S1 and S2† and plotted as a function of the surfactant concentration in Fig. 8. The both transition temperatures $T_{m,1}$ and $T_{m,2}$ shift together to low temperature, and arrive at their respective constants at about their cmc values, indicating the correlation of transition temperatures to their cmc values. The enthalpy change (ΔH_1) corresponding to the first transition decreases obviously as the $C_{12}C_SC_{12}Br_2$ concentration increases. It is interesting to note that ΔH_2 has an approximately constant value in the whole range of the $C_{12}C_SC_{12}Br_2$ concentration. The second peak always overlaps partially with the first peak, suggesting that the second transition happens closely after the first one.

Generally, a protein has only one endothermic peak in the heating process, referred as a thermal denaturation process. The corresponding integrated enthalpy represents the transition enthalpy from a native state to its denatured state. However, it is well known that α-CT tends to self-aggregation in aqueous solution and the aggregation number depends on pH value. At pH = 7.3 for our systems the protein is in monomer-hexamer equilibrium.[45] Therefore, it may go through two processes in the transition from its native to denatured state, that is, the dissociation of the aggregates and denaturation (or unfolding) of α-CT regardless of the presence or absence of $C_{12}C_SC_{12}Br_2$. The dissociation of protein aggregates often is endothermic contrary to the exothermic effect of its aggregation process.[44,46] The interaction of $C_{12}C_SC_{12}Br_2$ with α-CT makes the α-CT aggregates dissociate easily and makes α-CT denature at lower temperature. The less stability of α-CT should correlate to flexible conformations in the secondary structure from CD spectra in Fig. 7 and the tertiary structure from fluorescence spectra in Fig. 6 induced by the electrostatic interaction with cationic $C_{12}C_SC_{12}Br_2$.

3. Conclusions

The enzymatic superactivity of α-CT in the studied $C_{12}C_SC_{12}Br_2$ solutions appears always before their cmc, which is closely related to the specific electrostatic interaction between surfactant and enzyme. The larger headgroup's hydrophobicity and/or size can promote the superactivity.[6,7,13,17,18] This work demonstrates that the effect on the superactivity arises from the electrostatic attraction. The headgroup's charge density dominates the interaction strength and a moderate charge density is beneficial to activate the superactivity. For α-CT/$C_{12}C_SC_{12}Br_2$ systems, the superactivity increases as the spacer length increases. It also can be controlled by the oppositely charged surfactant SDS or anions HPO_4^{2-} in PBS and can achieve its maximum because of the partial charge neutralization of $C_{12}C_SC_{12}Br_2$ headgroups. The $C_{12}C_SC_{12}Br_2$ with a shorter spacer length has a larger headgroup's charge density, and thus needs more concentrated PBS or SDS to activate the maximum superactivity of α-CT. The endothermic enthalpy change ($\Delta(\Delta H_{obs}) > 0$) indicates that the enthalpy change of the interaction between surfactant and α-CT results mainly from the conformational change of α-CT, which corresponds exactly to the event of the superactivity. The intrinsic fluorescence spectra of α-CT before and after the surfactants' cmc indicate that the electrostatic interaction makes α-CT have more flexible tertiary structure[8,39] before the cmc, whereas after the cmc it leads to the flexible as well as slightly unfolding tertiary structure. The far-UV CD spectra characterizes the change in the secondary structure of α-helix, β-component and random coil of α-CT. The results indicate almost the same secondary structure as in the pure PBS (10 mmol L^{-1}) before the surfactant's cmc, but after the cmc, progressive enhancement of the negative band and wavelength redshift suggest partial unfolding of the secondary structure. The conformational instability of α-CT was confirmed also by DSC thermogram. The transition temperatures $T_{m,1}$ and $T_{m,2}$ and the corresponding enthalpy changes decrease as the concentration of $C_{12}C_SC_{12}Br_2$ increases before the cmc, indicating that the enzyme has a weakened structural stability, including the dissociation of the enzyme oligomers and the unfolding of the enzyme.[26,44–46]

To sum up, the gemini surfactants with different spacer length have an different impact on the secondary, tertiary, and even fourth structure of α-CT and therefore on its relative activity. The headgroup charge density plays a critical role among other complex factors. This study proposes a novel strategy for controlling the enzymatic superactivity with oppositely charged mixed surfactants.

4. Experimental section

4.1 Materials

Alfa-Chymotrypsin (α-CT, 1000 μ mg^{-1}, CAS:9004-07-3), 2-naphthyl acetate (2-NA, >98%) and dodecyltrimethylammonium bromide (DTAB, >99%), sodium dodecyl sulfate (SDS, 99.5%) were purchased from Aladdin, 2-naphthyl (2-N, >99%) from TCI, $Na_2HPO_4 \cdot 12H_2O$ and $NaH_2PO_4 \cdot 2H_2O$ (AR grade) from Sinopharm Chemical Reagent Co., and ethylene glycol (AR grade) from Tianli Chemical Reagent Co., Ltd. All the chemicals employed in this work were used as received. Phosphate buffer solution (PBS) of pH 7.3 was prepared by dissolving $Na_2HPO_4 \cdot 12H_2O$ and $NaH_2PO_4 \cdot 2H_2O$ in double-distilled water (conductivity 1.2×10^{-6} S cm^{-1}) produced by an Automatic Distiller (SZ-93, Shanghai, China) and all the aqueous solutions were prepared with the PBS of 10 mmol L^{-1} except specially emphasized ones. Alkanediyl-α,ω-bis(dimethyldodecylammonium bromide) ($C_{12}C_SC_{12}Br_2$, $S = 2$, 6, and 10, see Scheme S1†) was synthesized and purified in a purity >99% as described in our previous work.[47] All chemicals for $C_{12}C_SC_{12}Br_2$ synthesis were analytical grade.

4.2 Assessment for enzymatic activity of α-CT

The enzymatic activity of α-CT was assessed in the presence of surfactant or its absence by the initial hydrolysis rate of 2-NA in PBS. In order to make the substrate easy to dissolve in the used buffer solution, the stock solution of 2-NA was prepared by dissolving 2-NA in glycol to obtain a concentration of 6.00 mmol L^{-1} and kept away from light. The presence of glycol does not affect the enzymatic activity assessment because of its very low volume fraction of 3% (V_{glycol}/V_{total}), and no self-decomposition of 2-NA was detected by UV-vis spectrometry measurements during 24 h, which is similar to the case in glycerol solvent.[48] The enzymatic reaction was always triggered by the addition of substrate 2-NA. The reaction was monitored by the increase of 2-N absorbance as a function of time at a wavelength of 328 nm at 298.15 K, using TU-1900 UV-vis spectrophotometer (Beijing Purkinje GeneralInstrument Co., Ltd) with a cuvette stand controlled by a circular water thermostat. The initial reaction rate of 2-NA hydrolysis was obtained from the slope of the 2-N concentration *versus* time profile. All the experiments were performed at the constant concentrations of 0.10 g L^{-1} α-CT and 0.081 mmol L^{-1} 2-NA in the presence of various surfactant additives or in their absence. Except for the specific pronouncement, the concentration of phosphate buffer is 10 mmol L^{-1} and always has a pH of 7.3. The relative activity ν_r of α-CT was expressed as a ratio of the initial hydrolysis rate (ν_i) under the various environments to the initial rate (ν_0) in pure PBS. In blank experiment without α-CT no detectable product 2-N was found in 20 min in the absence or presence of the employed surfactants, so that the self-hydrolysis of 2-NA or the micellar catalysis can be safely ruled out. The results were always presented as the average value of triplicate measurements and the standard deviation is ±0.03.

4.3 Isothermal titration calorimetry (ITC)

An isothermal titration calorimeter (Part No 3410, 1 mL reaction vessels) with a Thermostat TAM III (4 channels, TA Instruments, USA) was used to determine the enthalpy of micellization of surfactant in buffer solution and the interaction enthalpy between α-CT and $C_{12}C_SC_{12}Br_2$ ($S = 2$, 6, and 10) or DTAB. The experiment was performed as previous description.[36] Briefly, a surfactant solution was automatically added into buffer or buffered α-CT solution in aliquots of 3–6 μL from a gas tight Hamilton syringe controlled by a precision syringe pump with a control module (P/N 3810-5) through a thin stainless steel capillary until the desired range of concentration had been covered. During the whole titration process, the system was stirred at 80 rpm with a gold propeller, and the interval between two injections was 8 min under a dynamic correction model for the output signal to return to the baseline. All results were presented in average value of parallel triple titrations at (298.15 ± 0.01) K.

4.4 Fluorescence spectroscopy

The fluorescence spectrum was recorded on LS 55 fluorescence spectrometer (Perkin Elmer, America) using a 10 mm path length cuvette with both the excitation and emission slits fixed at 5.0 nm. The excitation wavelength was set at 295 nm, and emission spectrum was recorded from 300 to 450 nm with a scan speed of 500 nm min^{-1} at 298.15 K.

4.5 Circular dichroism (CD) spectroscopy

Circular dichroism (CD) spectra of α-CT from 190 to 270 nm were collected on Chirascan spectrometer (Applied Photophysics Ltd, Chirascan) at 298 K using a 1.0 mm quartz cell with the scan speed of 50 nm min^{-1}. Both spectral bandwidth and data pitch were 1 nm. Three scans were recorded and averaged for each CD spectrum. The buffer baseline was subtracted from the observed CD spectra to eliminate the possible interference. The concentration of α-CT was 0.10 g L^{-1} (in PBS, pH 7.3). The CD spectra of α-CT were analyzed by CDNN software to estimate the secondary structure contents.

4.6 Differential scanning calorimetry (DSC)

The thermal stability of α-CT was studied by using a differential scanning calorimeter (GE MicroCal VP-DSC, USA). Two fixed cells with a volume of 0.529 mL were filled with sample solution and reference solution (10 mmol L^{-1} PBS), respectively. The solutions were degassed with MicroCal ThermoVac before injecting into the individual cell at room temperature. The samples were equilibrated at the starting temperature (15 °C) for 15 min, and then the scan was performed at a scanning rate of 70 °C h^{-1} from 15 °C to 85 °C. The baseline of buffer was obtained by running with the same buffer solutions in the both cells and subtracted from all the resulting thermograms.

Conflicts of interest

There are no conflicts to declare.

Acknowledgements

This work received support from the National Natural Science Foundation of China (Project Nos. 21773059, 51905158, 21873026).

References

1 (*a*) A. Singh, J. D. V. Hamme and O. P. Ward, *Biotechnol. Adv.*, 2007, **25**, 99–121; (*b*) D. Otzen, *Biochim. Biophys. Acta*, 2011, **1814**, 562–591; (*c*) M. Goldfeld, A. Malec, C. Podella and C. Rulison, *J. Pet. Environ. Biotechnol.*, 2015, **6**, 1000211; (*d*) T. A. Khan, H. Mahler and R. S. K. Kishore, *Eur. J. Pharm. Biopharm.*, 2015, **97**, 60–67; (*e*) M. Segal, R. Avinery, M. Buzhor, R. Shaharabani, A. Harnoy, E. Tirosh, R. Beck and R. J. Amir, *J. Am. Chem. Soc.*, 2017, **139**, 803–810; (*f*) N. Kamaly, B. Yameen, J. Wu and O. C. Farokhzad, *Chem. Rev.*, 2016, **116**, 2602–2663; (*g*) R. de la Rica, D. Aili and M. M. Stevens, *Adv. Drug Delivery Rev.*, 2012, **64**, 967–978.

2 (*a*) P. V. Iyer and L. Ananthanarayan, *Process Biochem.*, 2008, **43**, 1019–1032; (*b*) T. Nojima and T. Iyoda, *Angew. Chem., Int.*

Ed., 2017, **56**, 1308–1312; (*c*) T. E. Sintra, S. P. M. Ventura and J. A. P. Coutinho, *J. Mol. Catal. B: Enzym.*, 2014, **107**, 140–151.
3 (*a*) A. Sanchez-Fernandez, C. Diehl, J. E. Houston, A. E. Leung, J. P. Tellam, S. E. Rogers, S. Prevost, S. Ulvenlund, H. Sjögren and M. Wahlgren, *Nanoscale Adv.*, 2020, **2**, 4011–4023; (*b*) D. Winogradoff, S. John and A. Aksimentiev, *Nanoscale*, 2020, **12**, 5422–5434; (*c*) J. N. Pedersen, J. Lyngsø, T. Zinn, D. E. Otzen and J. S. Pedersen, *Chem. Sci.*, 2020, **11**, 699–712; (*d*) D. Saha, D. Ray, J. Kohlbrecher and V. K. Aswal, *ACS Omega*, 2018, **3**, 8260–8270.
4 E. Cunha, M. L. C. Passos, P. C. A. G. Pinto and M. L. M. F. S. Saraiva, *Colloids Surf., B*, 2014, **118**, 172–178.
5 E. Abuin, E. Lissi and C. Calderón, *J. Colloid Interface Sci.*, 2007, **308**, 573–576.
6 F. Alfani, M. Cantarella, N. Spreti, R. Germani and G. Savelli, *Appl. Biochem. Biotechnol.*, 2000, **88**, 1–15.
7 N. Spreti, F. Alfani, M. Cantarella, F. D'Amico, R. Germani and G. Savelli, *J. Mol. Catal. B: Enzym.*, 1999, **6**, 99–110.
8 M. S. Celej, M. G. Dandrea, P. T. Campana, G. D. Fidelio and M. L. Bianconi, *Biochem. J.*, 2004, **378**, 1059–1066.
9 E. Abuin, E. Lissi and R. Duarte, *J. Mol. Catal. B: Enzym.*, 2004, **31**, 83–85.
10 P. Viparelli, F. Alfani and M. Cantarella, *J. Mol. Catal. B: Enzym.*, 2003, **21**, 175–187.
11 R. Pitt-Rivers and F. S. A. Impiombato, *Biochem. J.*, 1968, **109**, 825–831.
12 J. A. Reynolds and C. Tanford, *Proc. Natl. Acad. Sci. U. S. A.*, 1970, **66**, 1002–1008.
13 P. Viparelli, F. Alfani and M. Cantarella, *J. Mol. Catal. B: Enzym.*, 2001, **15**, 1–8.
14 M. A. Biasutti, E. B. Abuin, J. J. Silber, N. M. Correa and E. A. Lissi, *Adv. Colloid Interface Sci.*, 2008, **136**, 1–24.
15 E. Abuin, E. Lissi and R. Duarte, *Langmuir*, 2003, **19**, 5374–5377.
16 E. Abuin, E. Lissi and R. Duarte, *J. Colloid Interface Sci.*, 2005, **283**, 539–543.
17 P. Viparelli, F. Alfani and M. Cantarella, *Biochem. J.*, 1999, **344**, 765–773.
18 K. K. Ghosh and S. K. Verma, *Int. J. Chem. Kinet.*, 2009, **41**, 377–381.
19 D. Das, S. Roy, R. N. Mitra, A. Dasgupta and P. K. Das, *Chem.–Eur. J.*, 2005, **11**, 4881–4889.
20 R. Nagarajan, *Langmuir*, 2002, **18**, 31–38.
21 S. Javadian and J. Kakemam, *J. Mol. Liq.*, 2017, **242**, 115–128.
22 S. Backlund, J. Sjoblom and E. Matijevibb, *Colloids Surf., A*, 1993, **79**, 263–273.
23 L. T. Okano, F. H. Quina and O. A. E. Seoud, *Langmuir*, 2000, **16**, 3119–3123.
24 Y. Liu, Y. Liu and R. Guo, *J. Colloid Interface Sci.*, 2010, **351**, 180–189.
25 M. N. Jones, *Chem. Soc. Rev.*, 1992, **21**, 127–136.
26 G. Bai, J. Liu, J. Wang, Y. Wang, Y. Li, Y. Zhao and M. Yao, *Acta Phys.-Chim. Sin.*, 2017, **33**, 976–983.
27 M. A. Mir, J. M. Khan, R. H. Khan, G. M. Rather and A. A. Dar, *Colloids Surf., B*, 2010, **77**, 54–59.
28 S. Mondal, S. Das and S. Ghosh, *J. Surfactants Deterg.*, 2015, **18**, 471–476.
29 S. K. Hait and S. P. Moulik, *Curr. Sci.*, 2002, **82**, 1101–1111.
30 M. J. Rosena and D. J. Tracy, *J. Surfactants Deterg.*, 1998, **1**, 547–553.
31 R. Zana and J. Xia, *Gemini Surfactants: synthesis, interfacial and solution-phase behavior, and applications, Surfactant science series*, Marcel Dekker, Inc., 2004, vol. 117.
32 S. K. Verma, B. K. Ghritlahre, K. K. Ghosh, R. Verma, S. Verma and X. ZHAO, *Int. J. Chem. Kinet.*, 2016, **48**, 779–784.
33 A. Patra, N. Samanta, D. K. Das and R. K. Mitra, *J. Phys. Chem. B*, 2017, **121**, 1457–1465.
34 N. Spreti, P. D. Profio, L. Marte, S. Bufali, L. Brinchi and G. Savelli, *Eur. J. Biochem.*, 2001, **268**, 6491–6497.
35 D. L. Nelson and M. M. Cox, *Lehninger Principles of Biochemistry*, W. H. Freeman and Company, New York, 4th edn, 2004.
36 (*a*) P. Lou, Y.-J. Wang, G. Bai, C. Fan and Y.-L. Wang, *Acta Phys.-Chim. Sin.*, 2013, **29**, 1401–1407; (*b*) Y. Wang, P. Lou, G. Bai, C. Fan and M. Bastos, *J. Chem. Thermodyn.*, 2014, **73**, 255–261; (*c*) G. Bai, Y. Wang, Y. Ding, K. Zhuo, J. Wang and M. Bastos, *J. Chem. Thermodyn.*, 2016, **94**, 221–229; (*d*) Z. Xing, Z. Guo, Y. Zhang, J. Liu, Y. Wang and G. Bai, *Acta Phys.-Chim. Sin.*, 2020, **36**, 190600629.
37 Y. Wang and E. F. Marques, *J. Mol. Liq.*, 2008, **142**, 136–142.
38 M. Akram, I. A. Bhat, S. Anwar and K. Din, *J. Mol. Liq.*, 2015, **212**, 641–649.
39 J. J. Birktoft and D. M. Brow, *J. Mol. Biol.*, 1972, **68**, 187–240.
40 J. G. Lees, A. J. Miles, F. Wien and B. A. Wallace, *Bioinformatics*, 2006, **22**, 1955–1962.
41 L. M. Simon, M. Kotorman, G. Garab and I. Laczko, *Biochem. Biophys. Res. Commun.*, 2001, **280**, 1367–1371.
42 P. Attri, P. Venkatesu and M. Lee, *J. Phys. Chem. B*, 2010, **114**, 1471–1478.
43 L. M. Simon, M. Kotorman, G. Garab and I. Laczko, *Biochem. Biophys. Res. Commun.*, 2002, **293**, 416–420.
44 M. Roberge, R. N. A. H. Lewis, F. Shareck, R. Morosoli, D. Kluepfel, C. Dupont and R. N. McElhaney, *Proteins: Struct., Funct., Genet.*, 2003, **50**, 341–354.
45 A. C. Hamill, S. Wang and C. T. Lee, *Biochem*, 2007, **46**, 7694–7705.
46 (*a*) J. Wen, K. Arthur, L. Chemmalil, S. Muzammil, J. Gabrielson and Y. Jiang, *J. Pharm. Sci.*, 2012, **101**, 955–965; (*b*) S. Abarova, R. Koynova, L. Tancheva and B. Tenchova, *Biochim. Biophys. Acta, Mol. Basis Dis.*, 2017, **1863**, 2934–2941.
47 Y. Wang, G. Bai, E. F. Marques and H. Yan, *J. Phys. Chem. B*, 2006, **110**, 5294–5300.
48 G. R. Castro, *Enzyme Microb. Technol.*, 2000, **27**, 143–150.